Radio Science, Volume ???, Number , Pages 1–24,

Comparison of Stochastic Methods for the Variability Assessment of Technology Parameters

P. Manfredi,[1] M. Fontana,[1] I. S. Stievano,[1] and F. G. Canavero[1]

P. Manfredi, M. Fontana, I. S. Stievano, F. G. Canavero, Dipartimento di Elettronica, Politecnico di Torino, Corso Duca degli Abruzzi 24, I-10129, Torino, Italy. ({paolo.manfredi,michele.fontana,igor.stievano,flavio.canavero}@polito.it)

[1]Dipartimento di Elettronica, Politecnico di Torino, Turin, Italy.

This paper provides and compares two alternative solutions for the simulation of cables and interconnects with the inclusion of the effects of parameter uncertainties, namely the Polynomial Chaos (PC) method and the Response Surface Modeling (RSM). The problem formulation applies to the telegraphers equations with stochastic coefficients. According to PC, the solution requires an expansion of the unknown parameters in terms of orthogonal polynomials of random variables. On the contrary, RSM is based on a least-square polynomial fitting of the system response. The proposed methods offer accuracy and improved efficiency in computing the parameter variability effects on system responses with respect to the conventional Monte Carlo approach. These approaches are validated by means of the application to the stochastic analysis of a commercial multiconductor flat cable. This analysis allows us to highlight the respective advantages and disadvantages of the presented methods.

1. Introduction

The constant and rapid pace of technological innovation today has produced increasingly complex electronic devices to such an extent that they are often physically separated into several sub-devices and then connected together. The integrity of signals propagating on interconnections is then a fundamental point for the smooth functioning of the overall system. Cable bundles represent one of the most common means by which modern electronic systems and subsystems are interconnected. A large variety of examples exists, ranging from transportation vehicles (cars, aircrafts, ships) to Information Technology equipment and to industrial plants. The electromagnetic interaction among closely spaced individual wires induces disturbances in all other adjacent circuits. This crosstalk can cause functional degradation of the circuits at the ends of the cable. The magnitude of the electromagnetic interference varies significantly as a function of a number of factors including the wires geometries.

The sensitivity of crosstalk to random wires position in the cable has led to several probabilistic models for the crosstalk according to the frequency ranges. Instead of using brute-force Monte Carlo (MC) method, some alternative solutions based on the derivation of pseudo-analytical expressions for the statistical parameters of the responses of distributed systems have been proposed so far [*Shiran at al.*, 1993; *Bellan et al.*, 2003]. However, their principal limitation is related to their scarce flexibility and restriction to the particular structures and output variables for which they have been derived. Possible complementary methods based on the optimal selection of the subset of model parameters in the whole design space [*Zhang et al.*, 2001] have

also been proposed. However, these methods turn out to be extremely inefficient, since they require a large set of simulations with different samples of the random parameters and prevent us from applying them to the analysis of complex realistic structures.

Recently, an effective solution based on the so-called polynomial chaos (PC) has been proposed to overcome the previous limitations. This methodology is based on the representation of the stochastic solution of a dynamical circuit in terms of orthogonal polynomials. For a comprehensive and formal discussion of PC theory, the reader is referred to [*Ghanen and Spanos*, 1991; *Xiu and Karniadakis*, 2002; *Debusschere et al.*, 2004] and references therein; also, it should be pointed out that the word *chaos* is used in the sense originally defined by Wiener [*Wiener*, 1938] as an approximation of a Gaussian random process by means of Hermite polynomials. This technique has been successfully applied to several problems in different domains, including the extension of the classical circuit analysis tools, like the modified nodal analysis (MNA), to the prediction of the stochastic behavior of circuits [*Strunz and Su*, 2008; *Zout et al.*, 2007; *Stievano and Canavero*, 2010]. However, so far, the application has been mainly focused on the gaussian variability of model parameters and limited to dynamical circuits consisting only of lumped elements. The authors of this contribution have recently proposed an extension of PC theory to distributed structures described by transmission-line equations [*Manfredi et al.*, 2010], also in presence of uniform random variables.

The main drawback of PC is related to the reduction of its efficiency when the number of random variables increases. A possible solution consists in performing preliminary tests to identify the most influential variables to be included in the model [*Manfredi and Canavero*, 2011]. Yet, an approach based on the Response Surface Modeling (RSM) is also possible and presented in this paper as an alternative to PC, followed by a comparison between the two methods. The RSM is based on the fitting of a system response using polynomial terms, whose coefficients are computed in a least-square sense starting from a reduced set of samples.

In order to be validated and compared, the advocated techniques are applied to the stochastic analysis of a commercial multiconductor flex-cable used for the communication between PCB cards.

2. Variability via Polynomial Chaos

This section outlines the PC method, focusing in particular on the application to transmission lines described by telegraphers equations and validating it against a traditional MC simulation on a commercial cable bundle. For further information, readers are referred to [*Manfredi et al.*, 2010] and references therein, where a more comprehensive and detailed discussion is available.

2.1. PC Primer

The idea underlying the PC technique is the spectral expansion of a stochastic function (intended as a given function of a random variable) in terms of a truncated series of orthogonal polynomials. Within this framework, a function H, that in

our specific application will be the expression of the parameters and the resulting frequency-domain response of an interconnect described as a transmission line, can be approximated by means of the following truncated series

$$H(\xi) = \sum_{k=0}^{P} H_k \cdot \phi_k(\xi), \tag{1}$$

where $\{\phi_k\}$ are suitable orthogonal polynomials expressed in terms of the random variable ξ. The above expression is defined by the class of the orthogonal bases, by the number of terms P and by the expansion coefficients H_k. The choice of the orthogonal basis relies on the distribution of the random variables being considered. The tolerances given in product documentation and datasheets are usually expressed in terms of minimum, maximum and typical values. Since the actual distribution is generally unknown, a reasonable assumption is to consider the parameters as random variables with uniform distribution between the minimum and maximum values. Hence, the most appropriate orthogonal functions for the expansion (1) are the Legendre polynomials, the first three being $\phi_0 = 1$, $\phi_1 = \xi$ and $\phi_2 = (\frac{3}{2}\xi^2 - \frac{1}{2})$, where ξ is the normalized uniform random variable with support $[-1, 1]$. It is relevant to remark that any random parameter in the system, e.g., a dielectric permittivity ε_r, can be related to ξ as follows

$$\varepsilon_r = \frac{b+a}{2} + \frac{b-a}{2}\xi, \tag{2}$$

where a and b are the minimum and maximum values assumed by the parameter, respectively. The orthogonality property of Legendre polynomials is expressed by

$$< \phi_k, \phi_j > = < \phi_k, \phi_k > \delta_{kj}, \tag{3}$$

where δ_{kj} is the Kronecker delta and $< \cdot, \cdot >$ denotes the inner product in the Hilbert space of the variable ξ with uniform weighting function, i.e.,

$$< \phi_k, \phi_j >= \frac{1}{2} \int_{-1}^{1} \phi_k(\xi)\phi_j(\xi)d\xi. \quad (4)$$

With the above definitions, the expansion coefficients H_k of (1) are computed via the projection of H onto the orthogonal components ϕ_k. It is worth noting that relation (1), which is a known nonlinear function of the random variable ξ, can be used to predict the probability density function (PDF) of $H(\xi)$ via numerical simulation or analytical formulae [*Papoulis*, 1991].

The basic results of PC theory outlined above can be extended to the case of multiple independent random variables. The application of orthogonality relations allows to build higher dimensional polynomials as the product combination of polynomials in one variable. As an example, Tab. 1 shows the first bivariate Legendre polynomials, up to the third order.

2.2. Application to Transmission-Line Equations

This section discusses the modification to the transmission-line equations, allowing to include the effects of the statistical variation of the per-unit-length (p.u.l.) parameters via the PC theory. For the sake of simplicity, the discussion is based on the multiconductor transmission-line structure shown in Fig. 1, that represents the typical problem of two wires whose heights above ground and separation are not known exactly, thus leading to a probabilistic definition of crosstalk between the wires.

In the structure of Fig. 1, the height h and the separation d are assumed to be defined by

$$\begin{cases} h &= \bar{h} + (\Delta_h/2)\xi_1 \\ d &= \bar{d} + (\Delta_d/2)\xi_2, \end{cases} \tag{5}$$

where ξ_1 and ξ_2 are independent normalized uniform random variables, with $\bar{h}_1$ and $\bar{d}$ mean values and Δ_h and Δ_d supports. It should be noted that these variations define different possible configurations for the wire couple of Fig. 1, but each configuration is still uniform along the propagation direction.

The electrical behavior in frequency-domain of the line of Fig. 1 is described by the well-known telegraph equations:

$$\frac{d}{dz}\begin{bmatrix} \mathbf{V}(z,s) \\ \mathbf{I}(z,s) \end{bmatrix} = -s \begin{bmatrix} 0 & \mathbf{L} \\ \mathbf{C} & 0 \end{bmatrix} \begin{bmatrix} \mathbf{V}(z,s) \\ \mathbf{I}(z,s) \end{bmatrix}, \tag{6}$$

where s is the Laplace variable, $\mathbf{V} = [V_1(z,s), V_2(z,s)]^T$ and $\mathbf{I} = [I_1(z,s), I_2(z,s)]^T$ are vectors collecting the voltage and current variables along the multiconductor line (z coordinate) and $\mathbf{C}$ and $\mathbf{L}$ are the p.u.l. capacitance and inductance matrices depending on the geometrical and material properties of the structure [*Paul*, 1994].

In order to account for the uncertainties affecting the guiding structure, we must consider the p.u.l. matrices $\mathbf{C}$ and $\mathbf{L}$ as random quantities, with entries depending on the random vector $\boldsymbol{\xi} = [\xi_1, \xi_2]^T$. In turn, (6) becomes a stochastic differential equation, leading to randomly-varying voltages and currents along the line.

For the current application, the random p.u.l. matrices in (6) are represented through the Legendre expansion as follows:

$$\mathbf{C} = \sum_{k=0}^{P} \mathbf{C}_k \cdot \phi_k(\boldsymbol{\xi}), \qquad \mathbf{L} = \sum_{k=0}^{P} \mathbf{L}_k \cdot \phi_k(\boldsymbol{\xi}), \tag{7}$$

where $\{\mathbf{C}_k\}$ and $\{\mathbf{L}_k\}$ are expansion coefficients matrices with respect to the orthogonal components $\{\phi_k\}$ defined in Tab. 1. For a given number of random variables n and order p of the expansion – that corresponds to the highest order of the polynomials in (7) and generally lies within the range 2 to 5 for practical applications – the total number of terms is

$$(P+1) = \frac{(n+p)!}{n!p!}, \tag{8}$$

that turns out to be equal to ten for the case $n = 2$ and $p = 3$.

The randomness of the p.u.l parameters reflects into stochastic values of the voltage and current unknowns and makes us decide to use expansions similar to (7) for the electrical variables. This yields a modified version of (6), whose second row is provided below in extended form for $P = 2$, as an exemplification

$$\begin{aligned} &\tfrac{d}{dz}[\mathbf{I}_0(z,s)\phi_0(\boldsymbol{\xi}) + \mathbf{I}_1(z,s)\phi_1(\boldsymbol{\xi}) + \mathbf{I}_2(z,s)\phi_2(\boldsymbol{\xi})] = -s[\mathbf{C}_0\phi_0(\boldsymbol{\xi}) + \\ &+\mathbf{C}_1\phi_1(\boldsymbol{\xi}) + \mathbf{C}_2\phi_2(\boldsymbol{\xi})][\mathbf{V}_0(z,s)\phi_0(\boldsymbol{\xi}) + \mathbf{V}_1(z,s)\phi_1(\boldsymbol{\xi}) + \mathbf{V}_2(z,s)\phi_2(\boldsymbol{\xi})], \end{aligned} \tag{9}$$

where the expansion coefficients of electrical variables are readily identifiable.

Projection of (9) on the first three Legendre polynomials leads to the following set of equations, where the explicit dependence on variables is dropped for notational convenience:

$$\begin{aligned} &\tfrac{d}{dz}(\mathbf{I}_0<\phi_0,\phi_j> + \mathbf{I}_1<\phi_1,\phi_j> + \mathbf{I}_2<\phi_2,\phi_j>) = -s(\mathbf{C}_0<\phi_0^2,\phi_j>\mathbf{V}_0 + \\ &+\mathbf{C}_0<\phi_0\phi_1,\phi_j>\mathbf{V}_1 + \ldots + \mathbf{C}_2<\phi_2^2,\phi_j>\mathbf{V}_2), \quad j = 0,1,2 \end{aligned} \tag{10}$$

The above equation, along with the companion relation arising from the first row of (6), can be further simplified by using the orthogonality relations for the computation of the inner products $<\phi_k,\phi_j>$ and $<\phi_k\phi_l,\phi_j>$, leading to the following augmented system, where the random variables collected in vector $\boldsymbol{\xi}$ do not appear,

due to the integration process:

$$\frac{d}{dz}\begin{bmatrix}\tilde{\mathbf{V}}(z,s)\\ \tilde{\mathbf{I}}(z,s)\end{bmatrix} = -s\begin{bmatrix}0 & \tilde{\mathbf{L}}\\ \tilde{\mathbf{C}} & 0\end{bmatrix}\begin{bmatrix}\tilde{\mathbf{V}}(z,s)\\ \tilde{\mathbf{I}}(z,s)\end{bmatrix}. \tag{11}$$

In the above equation, the new vectors $\tilde{\mathbf{V}} = [\mathbf{V}_0, \mathbf{V}_1, \mathbf{V}_2]^T$ and $\tilde{\mathbf{I}} = [\mathbf{I}_0, \mathbf{I}_1, \mathbf{I}_2]^T$ collect the coefficients of the PC expansion of the unknown variables. The new p.u.l. matrix $\tilde{\mathbf{C}}$ turns out to be

$$\tilde{\mathbf{C}} = \begin{bmatrix}\mathbf{C}_0 & \frac{1}{3}\mathbf{C}_1 & \frac{1}{5}\mathbf{C}_2\\ \mathbf{C}_1 & \mathbf{C}_0 + \frac{2}{5}\mathbf{C}_2 & \frac{2}{5}\mathbf{C}_1\\ \mathbf{C}_2 & \frac{2}{3}\mathbf{C}_1 & \mathbf{C}_0 + \frac{2}{7}\mathbf{C}_2\end{bmatrix}, \tag{12}$$

and a similar relation holds for matrix $\tilde{\mathbf{L}}$.

It is worth noting that (11) is analogous to (6) and plays the role of the set of equations of a multiconductor transmission line with a number of conductors that is $(P+1)$ times larger than those of the original line. It should be remarked that the increment of the equation number is not detrimental for the method, since for small values of P (as typically occurs in practice), the additional overhead in handling the augmented equations is much less than the time required to run a large number of MC simulations.

The extension of the proposed technique to different multiconductor structures possibly including losses and to a larger number of random variables is straightforward. For instance, the procedure to include losses amounts to including the resistance and conductance matrices in (6) and the corresponding augmented matrices in (11).

The solution of a transmission-line equation requires the definition of boundary conditions, such as the Thevenin equivalent networks depicted in Fig. 2, defining sources and loads. For the deterministic case, the simulation amounts to combining

the port electrical relations of the two terminal elements with the transmission-line equation, and solving the system. This is a standard procedure as illustrated for example in [*Paul*, 1994] (see Ch.s 4 and 5). The port equations of the terminations of Fig. 2 in the Laplace domain become

$$\begin{cases} \mathbf{V}_a(s) \;=\; \mathbf{E}(s) - \mathbf{Z}_S(s)\mathbf{I}_a(s) \\ \mathbf{V}_b(s) \;=\; \mathbf{Z}_L(s)\mathbf{I}_b(s), \end{cases} \tag{13}$$

where $\mathbf{Z}_S = \mathrm{diag}([Z_{S1}, Z_{S2}])$, $\mathbf{Z}_L = \mathrm{diag}([Z_{L1}, Z_{L2}])$ and $\mathbf{E} = [E_1, 0]^T$. Also, in the above equation, the port voltages and currents need to match the solutions of the differential equation (6) at line ends (e.g., $\mathbf{V}_a(s) = \mathbf{V}(z{=}0, s)$, $\mathbf{V}_b(s) = \mathbf{V}(z{=}\mathcal{L}, s)$).

Similarly, when the problem becomes stochastic, the augmented transmission-line equation (11) is used in place of (6) together with the projection of the characteristics of the source and the load elements (13) on the first P Legendre polynomials. It is worth noticing that in this specific example, no variability is included in the terminations and thus the augmented characteristics of the source and load turn out to have a diagonal structure.

Once the unknown voltage and currents are computed, the quantitative information on the spreading of circuit responses can be readily obtained from the analytical expression of the unknowns. As an example, the frequency-domain solution of the magnitude of voltage V_{a1} with $P = 2$, leads to $|V_{a1}(j\omega)| = |V_{a10}(j\omega)\phi_0(\boldsymbol{\xi}) + V_{a11}(j\omega)\phi_1(\boldsymbol{\xi}) + V_{a12}(j\omega)\phi_2(\boldsymbol{\xi})|$. As already outlined in the introduction, the above relation turns out to be a known nonlinear function of the random vector $\boldsymbol{\xi}$ that can be used to compute the PDF of $|V_{a1}(j\omega)|$ via standard techniques as numerical simulation or analytical formulae [*Papoulis*, 1991].

2.3. Validation

As a proof of the capabilities of the proposed technique, the analysis of the test structure depicted in Fig. 3 is presented. The structure represents a 0.050" High Flex Life Cable in a standard 9-wire configuration. Figure 3 collects both the key parameters defining the geometry of the wires as well as the information on the two-terminal circuit elements connected at the near-end of the cable. The cable length is 80 cm and the far-end terminations are defined by identical RC parallel elements ($R = 10\,\mathrm{k\Omega}$, $C = 10\,\mathrm{pF}$) connecting the wires #1,...,#8 to the reference wire #0.

In this example, the goal is to estimate the response variability of the near-end crosstalk between two adjacent wires in a bundle of many wires. As highlighted in Fig. 3, line #4 is energized by the voltage source E_S and the other lines are quiet and kept in the low state via the R_S resistances. From the official datasheet of the cable, tolerance limits regarding the separation between wires ($d_{ij} \in [48, 52]$ mils) and the overall radius of each wire including the dielectric coating ($r_{c,i} \in [16, 19]$ mils) are available. There is no information about the permittivity value ε_r of the PVC dielectric coating. Nevertheless, this value typically represents a primary source of uncertainty and therefore cannot be neglected; a possible realistic range is $\varepsilon_r \in [2.9, 4.1]$. In order to reduce the number of random variables included in the PC model, a reasonable choice is to assume that only the separations between the generator and the two adjacent wires are effective on crosstalk, as well as the permittivity. Therefore, the variability is considered to be provided by the relative permittivity ε_r of the coating and the separations d_{34} and d_{45} between the active and its immediately adjacent

lines. These quantities are assumed to behave as independent uniform random variables lying in the aforementioned ranges. All the other parameters are considered to be equal to their nominal values. For this comparison a third order PC expansion of the p.u.l. parameters is computed via numerical integration based on the method described in [*Paul*, 1994] (see Sec. 3.2.4 and cylindrical structures).

Figure 4 shows a comparison of the Bode plot (magnitude) of the transfer function $H(j\omega) = V_3(j\omega)/E_S$ defining the near-end crosstalk computed via the advocated PC method and determined by means of the MC procedure. The solid black thin curves of Fig. 4 represent the $\pm 3\sigma$ interval of the transfer function, where σ indicates the standard deviation, determined from the results of the proposed technique. For comparison, the deterministic response with nominal values of all parameters is reported in Fig. 4 as a solid black thick line; also, a limited set of MC simulations (100, out of the 40,000 runs, in order not to clutter the figure) are plotted as gray lines. Clearly, the thin curves of Fig. 4 provide a qualitative information of the spread of responses due to parameters uncertainty. A better quantitative prediction can be appreciated in Fig. 5, comparing the PDF of $|H(j\omega)|$ computed for different frequencies (circles) with the distribution obtained via the analytical PC expansion (squares). The frequencies selected for this comparison correspond to the dashed lines shown in Fig. 4. The good agreement between the actual and the predicted PDFs and, in particular, the accuracy in reproducing the tails and the large variability of non-uniform shapes of the reference distributions, confirm the potential of the proposed method. Moreover, it should be noted that the reference MC distribution is computed by con-

sidering 9 random variables, i.e., the permittivity and all the wire-to-wire separations. The good agreement between the curves allows us to conclude that the limited set of variables included in the PC model represented a smart choice. For this example, it is also clear that a PC expansion with $P = 3$ is already accurate enough to capture the dominant statistical information of the system response.

3. Variability via Response Surface Modeling

Although PC provides an accurate stochastic model, even at high frequencies, the amount of time taken by the overhead and by the solution of the augmented system rapidly grows with the number of polynomial terms. Hence, the indiscriminate inclusion of any possible random variable in the PC model may be critical for this method and should be avoided. The variables should be carefully chosen among the most influential instead. Nonetheless, an alternative and effective method for the inclusion of a higher number of random variables exists and it is provided by the RSM. This section introduces this alternative method and compares it against MC and PC solutions of the same cable configuration shown in Fig. 3.

3.1. RSM Primer

The Response Surface Model [*Myers and Montgomery*, 2002] is a polynomial function which approximates the input/output behaviour of a complex system; the model is a non-linear equation constructed by fitting observed responses and inputs via a least-square fitting technique and it is used to predict the system output in response to arbitrary combinations of input variables.

A second-order RSM has the following general form:

$$y = \beta_0 + \sum_{i=1}^{n} \beta_i x_i + \sum_{i=1}^{n} \beta_{ii} x_i^2 + \sum_{i=1}^{j-1} \sum_{j=2}^{n} \beta_{ij} x_i x_j, \tag{14}$$

where y is the system response, β_i and β_{ij} are the model fit coefficients, x_i are the system inputs and n is the number of independent input variables. Even if quadratic and interaction terms are introduced to model weak non-linearities, RSM is still a linear function of fit coefficients β, whose amount is equal to $k = 1 + 2n + n\,(n-1)\,/2$. Therefore they can be evaluated through a least-square fitting technique, which calculates the coefficients from the system response and inputs by minimizing the sum of the square errors.

A second-order RSM is chosen noticing that it is flexible enough to model the observed stochastic behavior. Although in the field of parametric modeling there are more complex and powerful approaches, e.g., surrogate modeling [*Gorissen et al.*, 2010], which are more capable of extracting information from a lower amount of computationally-expensive data samples, in our application the most important requirement is the inclusion of a higher number of random variables. Despite its relative structural simplicity, RSM turns out to be suitable for our purpose, featuring a good model accuracy compared to standard MC approach.

The set of samples used for model fitting is determined in order to obtain accurate response surfaces over a wide range; a Latin Hypercube Sampling (LHS) plan yields a randomized space-filling sample set, whose projections on each design space dimension are uniformly spread, modeling appropriately all experimental corners of the design space. Sample size r is increased, starting from $r = k$, until standard

model evaluation criteria, e.g. RMSE and coefficients of multiple determination R^2 and R^2_{adj} [*Morris and Mitchell*, 1995; *devore*, 2000], are satisfied on a separate sample subset.

3.2. Application to Stochastic Frequency-Domain Response

This section discusses the application of RSM to interconnects, like the one depicted in Figs. 1 and 2, with the inclusion of the effects of the statistical variation of geometrical and material parameters. The goal is to model the response variability of some output, for instance the transfer function $H(j\omega) = V_{a2}(j\omega)/E_1$, defining the near-end crosstalk, with a polynomial RSM using normalized random variables as inputs.

For the sake of simplicity, we start considering the influence of two parameters, described by uniform random variables ξ_1 and ξ_2. The second-order RSM of $|H(j\omega)|$ in dB scale is composed of $k = 6$ terms and takes the following form, according to (14):

$$\begin{aligned} |H(j\omega)|_{\mathrm{dB}} = |H_0(j\omega)|_{\mathrm{dB}} + \beta_1(\omega)\,\xi_1 + \beta_2(\omega)\,\xi_2 + \beta_{11}(\omega)\,\xi_1^2 + \\ + \beta_{22}(\omega)\,\xi_2^2 + \beta_{12}(\omega)\,\xi_1\xi_2, \end{aligned} \tag{15}$$

where β_0 is set equal to the nominal transfer function $|H_0(j\omega)|_{\mathrm{dB}}$ without any effect of parameter variability. The remaining five terms have to be estimated through a least square fitting technique; it is relevant to remark that the system response and therefore model coefficients are frequency-dependent, hence a least square problem has to be solved for each frequency point. The choice of normalized random variables with support $[-1, 1]$ as inputs and of the magnitude of the transfer function in dB

as output reduces the variation of the fit coefficients, thus avoiding numerical instabilities in the model. However, a Response Surface Model for the estimation of the linear magnitude or phase may be created as well. It has been experimentally proven that a LHS-based design for $n = 2$ input variables requires a total of $r = 10$ samples, which are obtained from the solutions of line equation (6) computed for the values of the input variables specified by the sampling plan.

Once the fit coefficients are determined, the RSM represents an analytical function of the random variables (similarly to the case discussed earlier for the PC expansion), and it can be used to compute the PDF of $|H(j\omega)|_{\mathrm{dB}}$ through standard techniques. It is worth noting that the time required to evaluate the function output is much smaller than a single MC simulation, and this motivates the use of the proposed technique for a significantly large number of random variables.

3.3. Validation

This section refers to the stochastic analysis of the test structure already presented in Section 2.3, extending the considered variability to other parameters. A first RSM of $|H(j\omega)|_{\mathrm{dB}}$ is built considering $n = 9$ random variables as inputs, in order to include the variability of each wire-to-wire separation d_{ij}, as well as of the relative dielectric constant. The resulting polynomial function needs $k = 55$ terms, whose fit coefficients are estimated evaluating deterministic responses for a LHS composed of $r = 250$ samples.

Fig. 5 additionally shows the PDF obtained from the RSM. Again, the good correspondance demonstrates that RSM is indeed capable of handling a larger number of variables, assuring a good accuracy.

Moreover, a second RSM is created to perform a complete stochastic analysis of the structure, including also the thickness of wire insulators. Hence, the new model contains a total number of $n = 18$ variables, i.e., 8 wire-to-wire separations, 9 coating radii and the dielectric permittivity. To estimate the $k = 190$ fit coefficients of the polynomial function, a LHS composed of $r = 600$ samples is used. Fig. 6 shows the PDF of $|H(j\omega)|$ computed via MC simulations and by means of RSM polynomial function. The good agreement confirms that second-order Response Surface Models are sufficient to capture the non-uniform distribution of the statistical responses of this class of structures, when affected by a large number of random parameters.

4. Conclusions

This paper presents two alternative methods enabling to compute quantitative information on the sensitivity to parameters uncertainties of complex distributed interconnects described by multiconductor transmission-line equations.

PC is based on the expansion of the voltage and current variables into a sum of a limited number of orthogonal polynomials. It is shown that it provides very high accuracy when compared to conventional solutions like Monte Carlo in the evaluation of statistical parameters, even at high frequencies. Besides, PC allows to build a stand-alone (augmented) model describing an interconnect affected by parameters

variability. This model can be reused when simulating different test conditions, such as different loads and line lengths, as well as it can be integrated into more complex systems. However, it suffers from a loss of computational efficiency when the number of included random variables is raised.

RSM represents an alternative solution to overcome the previous limitation and it is based on a polynomial fitting of the desired output variables in a least-square sense. Yet, the model is limited to the specific conditions for which it is computed, and it needs to be re-built whenever the loads or the line length change. Typically, it is less accurate since some interaction terms are neglected to limit the amount of samples required.

Both methods have been applied to the stochastic analysis of a commercial multiconductor flex cable with uncertain parameters described by independent uniform random variables. Table 2 collects the main figures on the efficiency of the proposed methods vs. the conventional MC for a 300-point frequency sweep. It is worth noting that the setup time refers to the computation of the expansion and the augmented matrices for the PC case, while it refers to the computation of the solutions at sampling plan points for the RSM model. Table 2 data indicate that the PC and RSM computation of curves like those in Figs. 5 and 6 on the whole frequency range is faster by a factor ranging between 50 and 150 with respect to MC computation. This holds even if for fairness we consider the computational overhead required by the generation of the proposed models. Additionally, thanks to the analytical model provided by either PC or RSM, designers might achieve superior insight into the

354 influence of each system parameter, compared to the relatively blind MC approach.
355 This comparison confirms the strength of the proposed methods, that allow to gen-
356 erate accurate predictions of the statistical behavior of a realistic interconnect with
357 a great efficiency improvement.

References

358 Bellan, D., S. A. Pignari, and G. Spadacini (2003), Characterisation of Crosstalk in
359 Terms of Mean Value and Standard Deviation, *IEE Proceedings - Science, Mea-*
360 *surement and Technology, 150(6)*, 289–295, doi:10.1049/ip-smt:20030968.

361 Debusschere B. J., H. N. Najm, P. P. Pébay, O. M. Knio, R. G. Ghanem, and
362 O. P. Le Maître (2004), Numerical Challenges in the Use of Polynomial Chaos
363 Representations for Stochastic Processes, *SIAM Journal on Scientific Computing,*
364 *26(2)*, 698–719.

365 Devore, J. L. (2000), *Probability and Statistics for Engineers and the Sciences,*
366 Duxbury.

367 Ghanen, R. G., and P. D. Spanos (1991), *Stochastic Finite Elements. A Spectral*
368 *Approach,* Springer-Verlag.

369 Manfredi, P., and F. G. Canavero (2011), Polynomial Chaos-Based Toler-
370 ance Analysis of Microwave Planar Guiding Structures, *Digest of 2011 IEEE*
371 *MTT-S International Microwave Symposium,* Baltimore, MD, U.S.A., 1–4,
372 doi:10.1109/MWSYM.2011.5972809.

Manfredi, P., I. S. Stievano, and F. G. Canavero (2010), Parameters Variability Effects on Microstrip Interconnects via Hermite Polynomial Chaos, *Proc. of 19th IEEE Conference on Electrical Performance of Electronic Packaging and Systems,* Austin, TX, U.S.A., 149–152, doi:10.1109/EPEPS.2010.5642568.

Myers, R. H., and D. C. Montgomery (2002), *Response Surface Methodology,* Wiley.

Gorissen, D., K. Crombecq, I. Couckuyt, T. Dhaene, and P. Demeester (2010), A Surrogate Modeling and Adaptive Sampling Toolbox for Computer Based Design, *Journal of Machine Learning Research, 11*, 2051–2055.

Morris, M. D., and T. J. Mitchell (1995), Exploratory Designs for Computational Experiments, *Journal of Statistical Planning and Inference, 43*, 381–402.

Papoulis, A. (1991), *Probability, Random Variables and Stochastic Processes,* 3rd edition, McGraw-Hill.

Paul, C. R. (1994), *Analysis of Multiconductor Transmission Lines,* Wiley.

Shiran, S., B. Reiser, and H. Cory (1993), A Probabilistic Model for the Evaluation of Coupling Between Transmission Lines, *IEEE Transactions on Electromagnetic Compatibility, 35(3)*, 387–393, doi:10.1109/15.277313.

Stievano, I. S., and F. G. Canavero (2010), Response Variability of High-Speed Interconnects via Hermite Polynomial Chaos, *Proc. of 14th IEEE Workshop on Signal Propagation on Interconnects,* Hildesheim, Germany, 3–6, doi:10.1109/SPI.2010.5483597.

Strunz, K., and Q. Su (2008), Stochastic Formulation of SPICE-Type Electronic Circuit Simulation Using Polynomial Chaos, *ACM Transactions on Modeling and*

Computer Simulation, 18(4), 15:1–15:23.

Wiener, N. (1938), The Homogeneous Chaos, *Amer. J. Math., 60*, 897–936.

Xiu, D., and G. E. Karniadakis (2002), The Wiener-Askey Polynomial Chaos for Stochastic Differential Equations, *SIAM, Journal of Sci. Computation, 24(2)*, 619–622.

Zhang, Q., J. J. Liou, J. McMacken, J. Thomson, and P. Layman (2001), Development of Robust Interconnect Model Based on Design of Experiments and Multiobjective Optimization, *IEEE Transactions on Electron Devices, 48(9)*, 1885–1891, doi:10.1109/16.944173.

Zou, Y., Y. Cai, Q. Zhou, X. Hong, S. H.-D. Tan, and L. Kang (2007), Practical Implementation of Stochastic Parameterized Model Order Reduction via Hermite Polynomial Chaos, *Proc. of 12th Asia and South Pacific Design Automation Conference,* Yokohama, Japan, 367–372, doi:10.1109/ASPDAC.2007.358013.

Figure captions

Figure 1. Cross-section of two coupled wires, whose height above ground and separation are uncertain parameters.

Figure 2. Definition of Thevenin equivalent boundary conditions at source and load terminations.

Figure 3. Application test structure: 80-cm long commercial flex cable (.050" High Flex Life Cable, 28 AWG Standard, PVC, 9-wire configuration). $R_S = 50\,\Omega$,

$d_w = 15\,\text{mils}$, $d_c = 35\,\text{mils}$. The nominal value of the distance between adjacent wires (e.g., d_{34} and d_{45}) is 50 mils.

Figure 4. Bode plots (magnitude) of the near-end crosstalk transfer function $H(j\omega)$ of the example test case (see text for details). Solid black thick line: deterministic response; solid black thin lines: 3σ tolerance limit of the third order polynomial chaos expansion; gray lines: a sample of responses obtained by means of the MC method (limited to 100 curves, for graph readability).

Figure 5. Probability density function of $|H(j\omega)|$ for the example of this study, computed at different frequencies. Of the three distributions, the one marked PC (3) refers to the response obtained via a third-order polynomial chaos expansion with 3 random variables, the one marked RSM (9) is generated from a second-order Response Surface Model including 9 random variables, while the one marked MC (9) refers to 40,000 MC simulations, involving the same nine variables of the RSM.

Figure 6. Probability density function of $|H(j\omega)|$ resulting from the variability of 18 independent parameters. Of the two distributions, the one marked RSM refers to the response obtained via second-order Response Surface Model, and the one marked MC refers to 40,000 MC simulations.

Table 1. Legendre Polynomials for the case of two independent random variables ($\boldsymbol{\xi} = [\xi_1, \xi_2]^T$) and a third-order expansion ($p = 3$).

index k	order p	k-th basis ϕ_k	$< \phi_k, \phi_k >$
0	0	1	1
1	1	ξ_1	$\frac{1}{3}$
2	1	ξ_2	$\frac{1}{3}$
3	2	$\frac{3}{2}\xi_1^2 - \frac{1}{2}$	$\frac{1}{5}$
4	2	$\xi_1\xi_2$	$\frac{1}{9}$
5	2	$\frac{3}{2}\xi_2^2 - \frac{1}{2}$	$\frac{1}{5}$
6	3	$\frac{5}{2}\xi_1^3 - \frac{3}{2}\xi_1$	$\frac{1}{7}$
7	3	$\frac{3}{2}\xi_1^2\xi_2 - \frac{1}{2}\xi_2$	$\frac{1}{15}$
8	3	$\frac{3}{2}\xi_1\xi_2^2 - \frac{1}{2}\xi_1$	$\frac{1}{15}$
9	3	$\frac{5}{2}\xi_2^3 - \frac{3}{2}\xi_2$	$\frac{1}{7}$

Table 2. CPU time required for the simulation of the setup of Fig. 3 by the standard MC method and the advocated PC and RSM techniques. See text for explanation of colums.

Method	# of random variables	Order	Setup	Simulation time	Speed-up
MC	–	–	–	3 h 53 min	–
PC	3	2	4.1 sec	1 min 50 sec	116×
PC	3	3	5 sec	4 min 20 sec	52×
RSM	9	2	1 min 23 sec	2.6 sec	163×
RSM	18	2	3 min 20 sec	21.7 sec	63×

Figure 1. Cross-section of two coupled wires, whose height above ground and separation are uncertain parameters.

Figure 2. Definition of Thevenin equivalent boundary conditions at source and load terminations.

Figure 3. Application test structure: 80-cm long commercial flex cable (.050" High Flex Life Cable, 28 AWG Standard, PVC, 9-wire configuration). $R_S = 50\,\Omega$, $d_w = 15\,\text{mils}$, $d_c = 35\,\text{mils}$. The nominal value of the distance between adjacent wires (e.g., d_{34} and d_{45}) is 50 mils.

Figure 4. Bode plots (magnitude) of the near-end crosstalk transfer function $H(j\omega)$ of the example test case (see text for details). Solid black thick line: deterministic response; solid black thin lines: 3σ tolerance limit of the third order polynomial chaos expansion; gray lines: a sample of responses obtained by means of the MC method (limited to 100 curves, for graph readability).

Figure 5. Probability density function of $|H(j\omega)|$ for the example of this study, computed at different frequencies. Of the three distributions, the one marked PC (3) refers to the response obtained via a third-order polynomial chaos expansion with 3 random variables, the one marked RSM (9) is generated from a second-order Response Surface Model including 9 random variables, while the one marked MC (9) refers to 40,000 MC simulations, involving the same nine variables of the RSM.

Figure 6. Probability density function of $|H(j\omega)|$ resulting from the variability of 18 independent parameters. Of the two distributions, the one marked RSM refers to the response obtained via second-order Response Surface Model, and the one marked MC refers to 40,000 MC simulations.

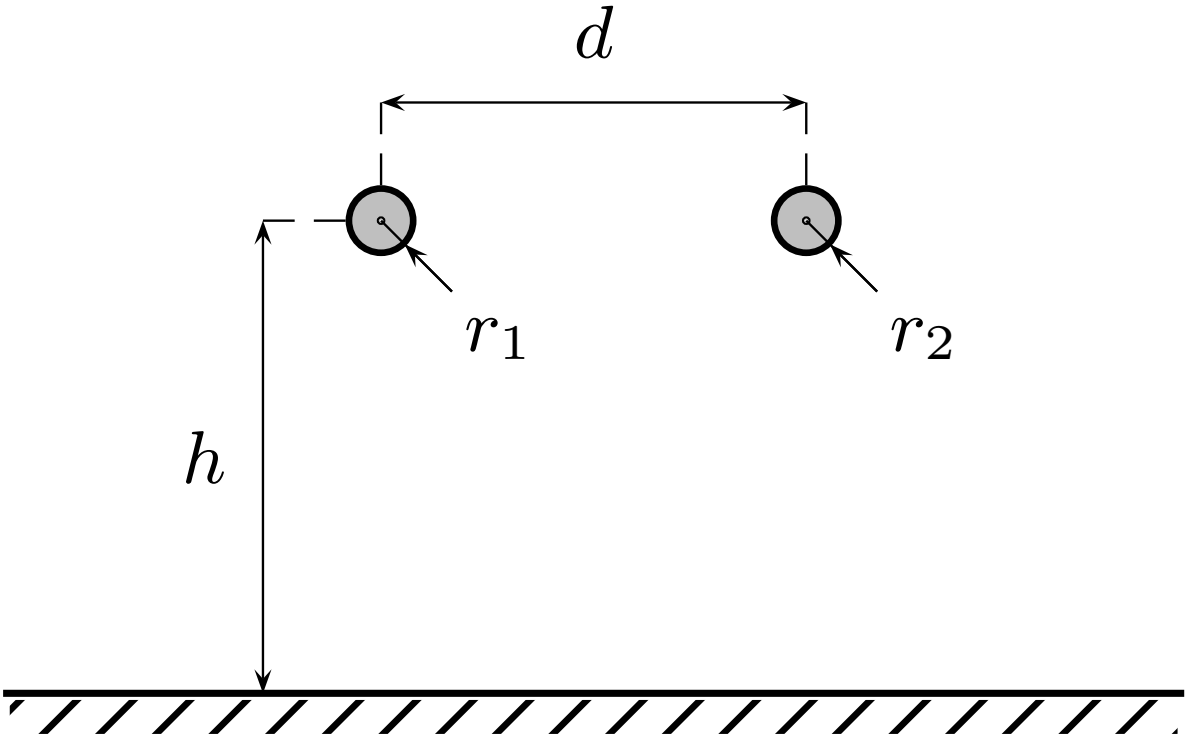
d
r1
r2
h

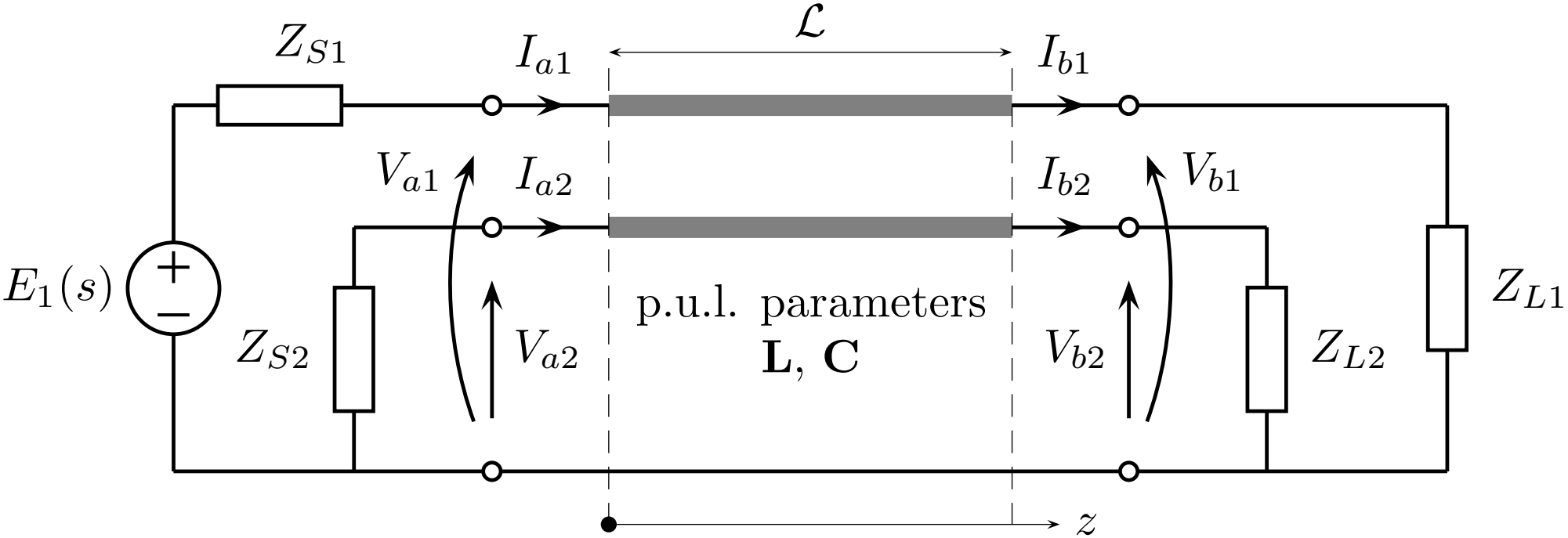
$\mathcal{L}$
Z_{S1}
I_{a1}
I_{b1}
V_{a1}
I_{a2}
I_{b2}
V_{b1}
$E_1(s)$
Z_{S2}
V_{a2}
p.u.l. parameters
L, **C**
V_{b2}
Z_{L2}
Z_{L1}
z

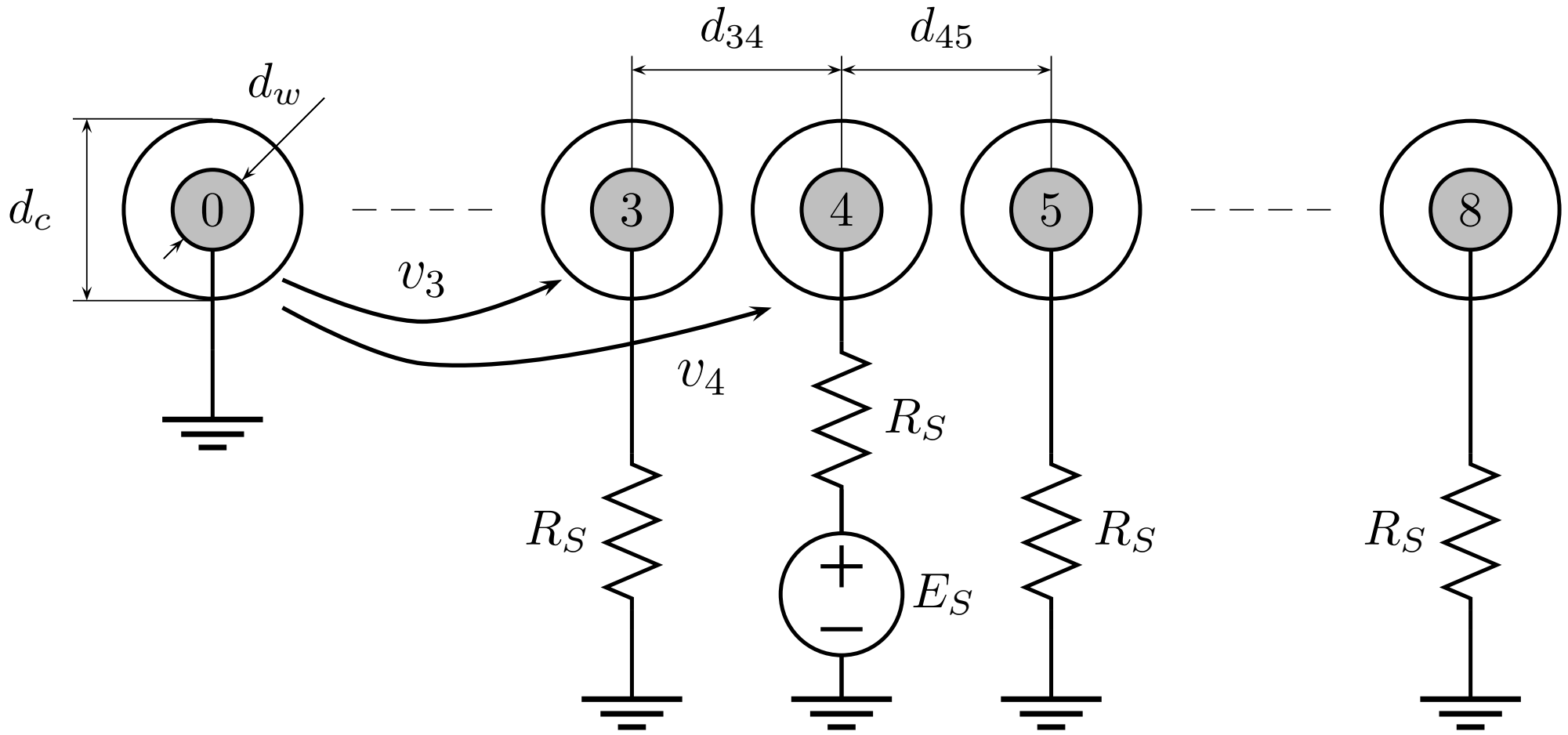
d_{34}
d_{45}
d_w
d_c
0
3
4
5
8
v_3
v_4
R_S
R_S
R_S
R_S
E_S

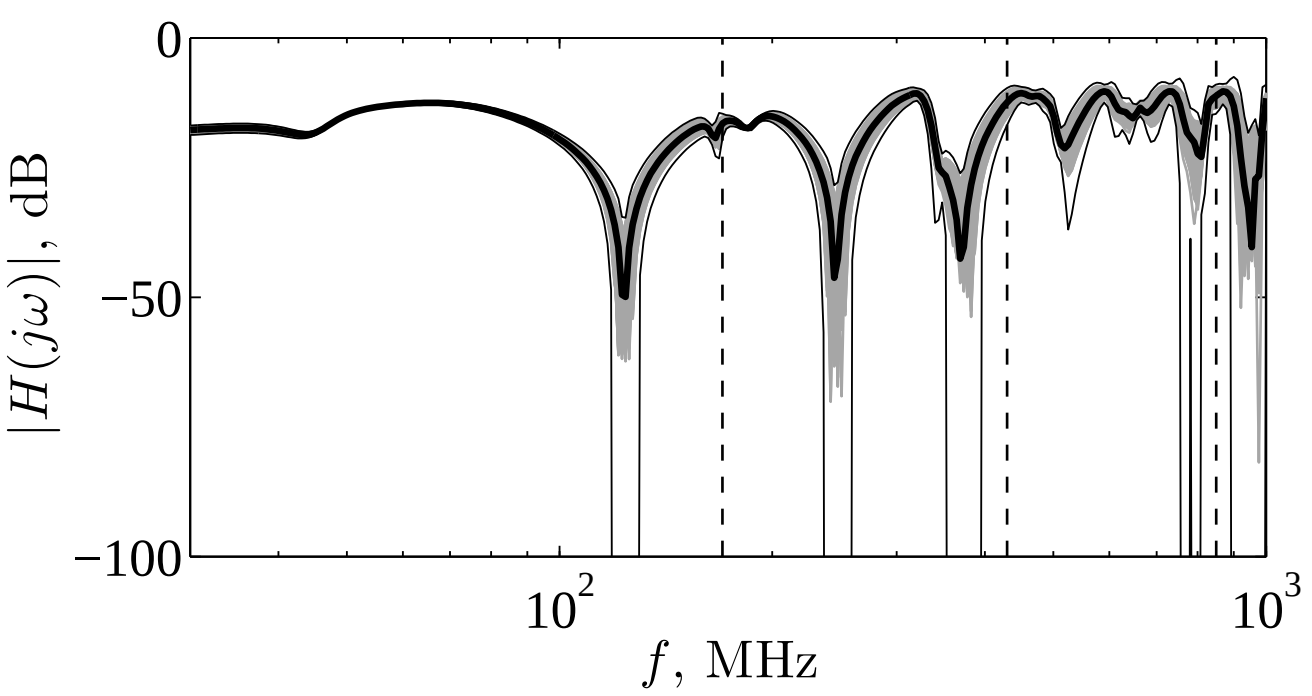
0
−50
−100
$|H(j\omega)|$, dB
10^2
10^3
f, MHz

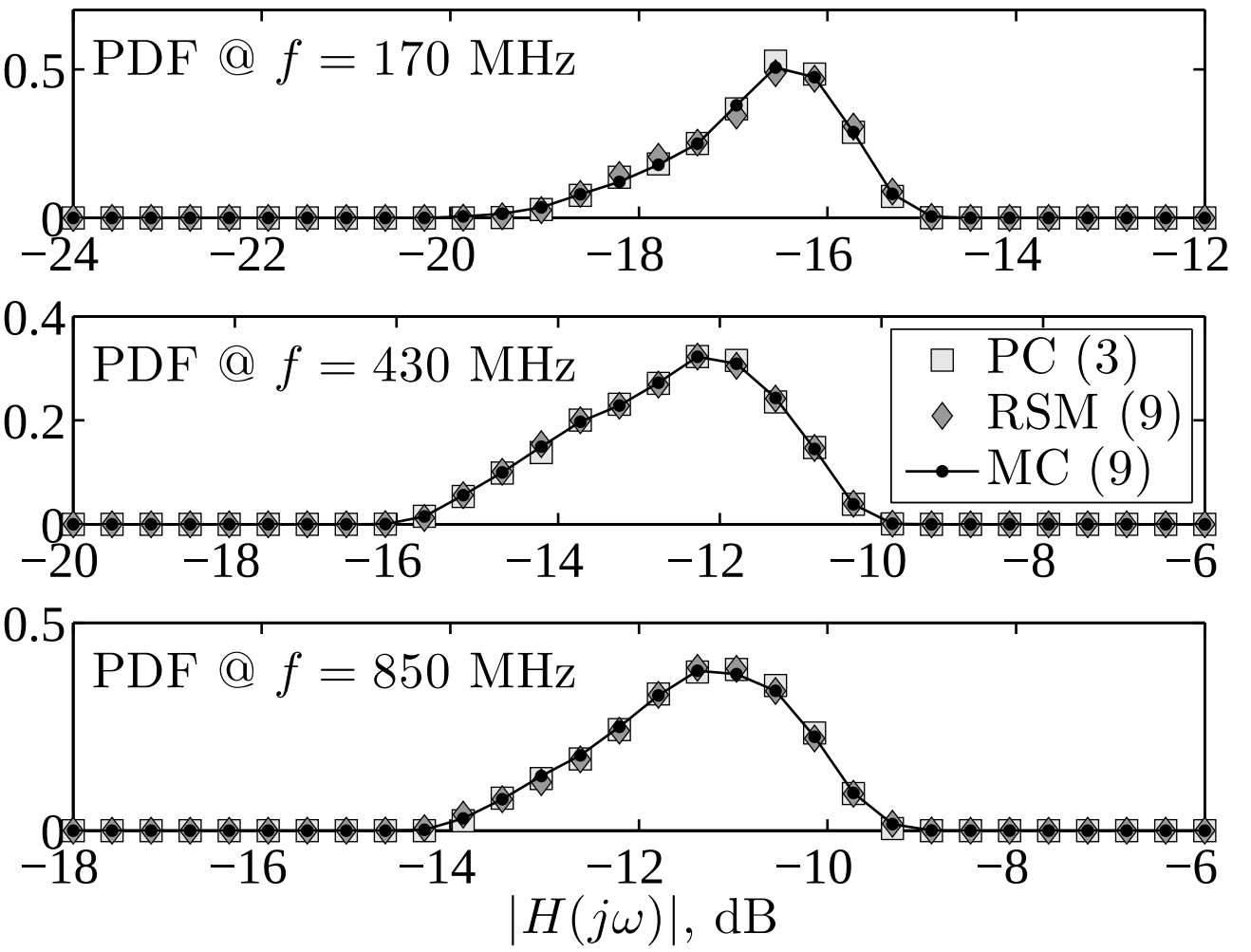
PDF @ $f = 170$ MHz
PDF @ $f = 430$ MHz
PDF @ $f = 850$ MHz
PC (3)
RSM (9)
MC (9)
$|H(j\omega)|$, dB

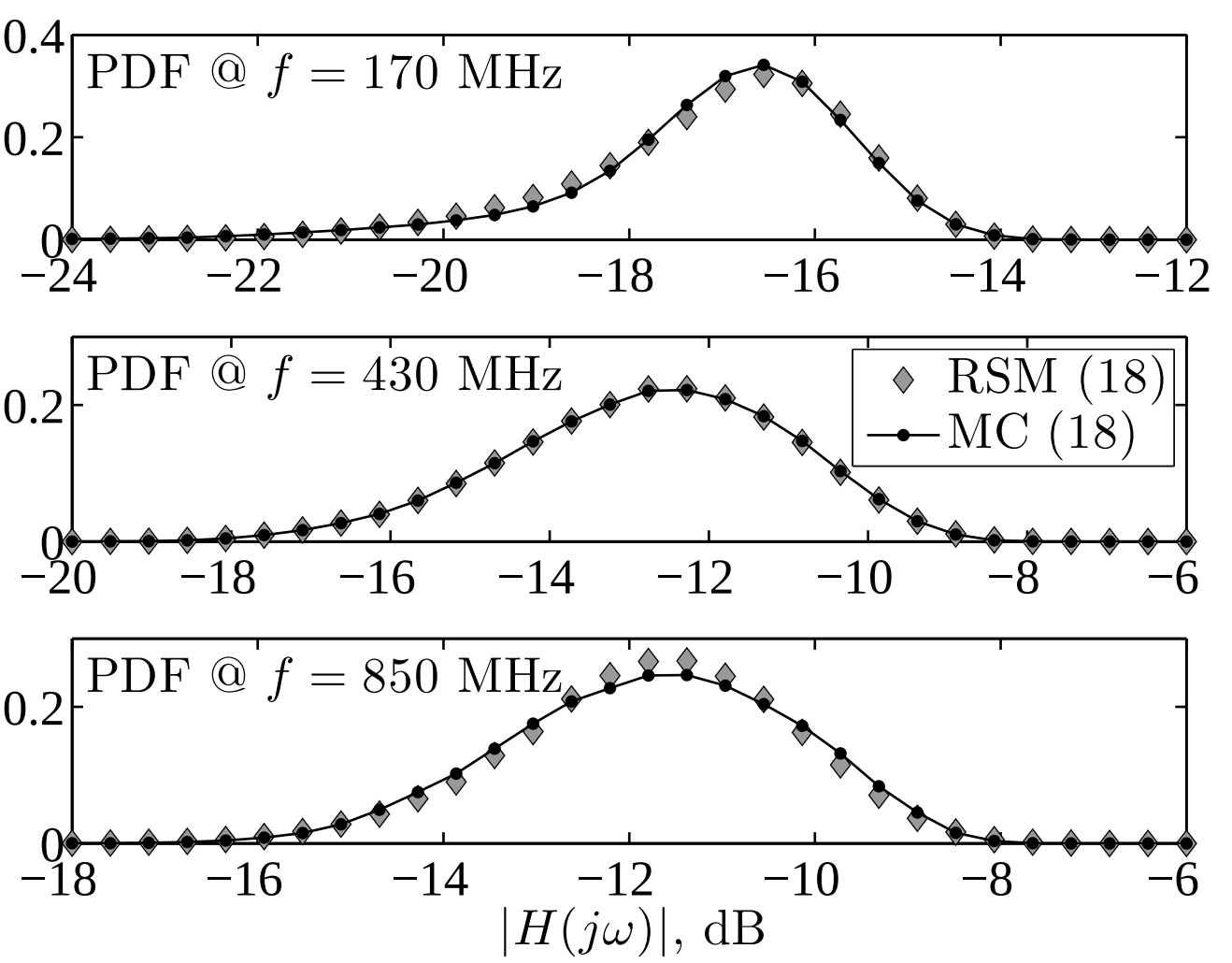
PDF @ $f = 170$ MHz
PDF @ $f = 430$ MHz
PDF @ $f = 850$ MHz
RSM (18)
MC (18)
$|H(j\omega)|$, dB